

Isoscalar and isovector kaon form factors from e^+e^- and τ data

Konstantin Beloborodov^{1,2,*}, Vladimir Druzhinin^{1,2}, and Sergey Serednyakov^{1,2}

¹Budker Institute of Nuclear Physics, 630090 Novosibirsk, Russia

²Novosibirsk State University, 630090 Novosibirsk, Russia

Abstract. The recent precise measurements of the $e^+e^- \rightarrow K_S K_L$ and $e^+e^- \rightarrow K^+K^-$ cross sections and the hadronic spectral function of the $\tau^- \rightarrow K^- K_S \nu_\tau$ decay are used to extract the isoscalar and isovector electromagnetic kaon form factors and their relative phase in a model independent way. The experimental results are compared with a fit based on the vector-meson-dominance model.

1 Introduction

Kaon electromagnetic form factors are the key objects in hadron physics describing electromagnetic interaction of kaons and providing important information about their internal structure.

In the timelike momentum-transfer region the form factors are usually extracted from experimental data on the reactions $e^+e^- \rightarrow K_S K_L$ and $e^+e^- \rightarrow K^+K^-$. In the resonance region at center-of-mass (c.m.) energies $\sqrt{s} < 2$ GeV, which we discuss in this paper, a substantial improvement in the accuracy of these cross sections was achieved in the recent measurements in the BABAR [1, 2], SND [3], and CMD-3 experiments [4, 5]. BABAR measured the $e^+e^- \rightarrow K^+K^-$ and the $e^+e^- \rightarrow K_S K_L$ cross sections using the initial-state-radiation method at the c.m. energies $\sqrt{s} = 0.98 - 4.85$ GeV and $\sqrt{s} = 1.08 - 2.16$ GeV, respectively. The SND and CMD-3 experiments used a direct scan. CMD-3 studied both the processes in the energy region near the ϕ -meson peak, while SND measured the $e^+e^- \rightarrow K^+K^-$ cross section in the range $\sqrt{s} = 1.05 - 2.00$ GeV. New data are expected from the SND and CMD-3 experiments soon.

The K^+K^- and $K_S K_L$ production Born cross sections are parametrized in terms of the charged and neutral kaon form factors as follows

$$\sigma_{K^+K^-}(s) = \frac{\pi\alpha^2\beta^3}{3s} |F_{K^+}|^2 C_{FS}(s), \quad (1)$$

$$\sigma_{K_S K_L}(s) = \frac{\pi\alpha^2\beta^3}{3s} |F_{K^0}|^2, \quad (2)$$

where $\beta = \sqrt{1 - 4m_{K^{(0)}}^2/s}$, and m_{K^-} and m_{K^0} are the charged and neutral kaon masses for Eqs. (1) and (2), respectively. The factor C_{FS} is the final state correction (see, e.g., Ref. [6]). This correction has significant deviation from unity only in a narrow interval near K^+K^-

*e-mail: K.I.Beloborodov@inp.nsk.su

threshold. The form factors F_{K^+} and F_{K^0} can be presented as a sum of the isoscalar and isovector parts:

$$F_{K^+} = F_{K^+}^{I=1} + F_{K^+}^{I=0}, \quad (3)$$

$$F_{K^0} = F_{K^0}^{I=1} + F_{K^0}^{I=0}. \quad (4)$$

The isospin invariance gives following relations between amplitudes for charged and neutral kaons [7]

$$F_{K^0}^{I=0} = F_{K^+}^{I=0}, \quad (5)$$

$$F_{K^0}^{I=1} = -F_{K^+}^{I=1}. \quad (6)$$

With this relations the cross sections proportional to squared moduli of the charged and neutral form factors can be expressed in term of isovector and isoscalar form factors $F_{K^+}^{I=0}$ and $F_{K^+}^{I=1}$

$$|F_{K^+}|^2 = |F_{K^+}^{I=1}|^2 + 2|F_{K^+}^{I=1}||F_{K^+}^{I=0}|\cos(\Delta\phi_{K^+}) + |F_{K^+}^{I=0}|^2, \quad (7)$$

$$|F_{K^0}|^2 = |F_{K^+}^{I=1}|^2 - 2|F_{K^+}^{I=1}||F_{K^+}^{I=0}|\cos(\Delta\phi_{K^+}) + |F_{K^+}^{I=0}|^2, \quad (8)$$

where $\Delta\phi_{K^+} = \phi_{K^+}^{I=1} - \phi_{K^+}^{I=0}$ is a relative phase between the isoscalar and isovector form factors. It is seen that data on the $e^+e^- \rightarrow K_S K_L$ and $e^+e^- \rightarrow K^+ K^-$ cross sections do not allow to separate the isovector and isoscalar contributions in a model-independent way. However, additional experimental information can be obtained from the $\tau^- \rightarrow K^- K^0 \nu_\tau$ decay under the conserved-vector-current (CVC) hypothesis. Recently, the precision measurement of the hadronic spectrum in this decay was performed by the BABAR collaboration [8].

The $\tau^- \rightarrow K^- K^0 \nu_\tau$ differential decay rate as a function of the $K^- K^0$ invariant mass M normalized to the τ leptonic width can be written as follows:

$$\frac{d\mathcal{B}(\tau^- \rightarrow K^- K^0 \nu_\tau)}{\mathcal{B}(\tau^- \rightarrow \mu^- \bar{\nu}_\mu \nu_\tau) M dM} = \frac{|V_{ud}|^2 S_{EW}}{2m_\tau^2} \left(1 + \frac{2M^2}{m_\tau^2}\right) \left(1 - \frac{M^2}{m_\tau^2}\right)^2 \beta_-^3 |F_{K^- K^0}(M)|^2, \quad (9)$$

where $|V_{ud}| = 0.97420 \pm 0.00021$ [9] is the Cabibbo-Kobayashi-Maskawa matrix element, $S_{EW} = 1.0235 \pm 0.003$ [10] is the short-distance electroweak correction, and $\beta_- = \sqrt{(1 - (m_{K^-} + m_{K^0})^2/M^2)(1 - (m_{K^-} - m_{K^0})^2/M^2)}$. Here we introduce the form factor $F_{K^- K^0}$. The CVC hypothesis in the limit of the isospin invariance give the relation between this form factor and the isovector electromagnetic form factor defined above [7]

$$F_{K^- K^0} = -2F_{K^+}^{I=1}. \quad (10)$$

It is tested for the $\tau^- \rightarrow \pi^- \pi^0 \nu_\tau$ decay that the CVC hypothesis works with a few percent accuracy without introducing other isospin-breaking corrections [11].

Finally, using data on the $e^+e^- \rightarrow K_S K_L$ and $e^+e^- \rightarrow K^+ K^-$ cross sections and the hadronic spectral function in the $\tau^- \rightarrow K^- K^0 \nu_\tau$ decay we can separate the isoscalar and isovector contributions and determine the moduli of the isoscalar and isovector form factors and the cosine of their relative phase:

$$\begin{aligned} |F_{K^+}^{I=1}|^2 &= 4|F_{K^- K^0}|^2, \\ |F_{K^+}^{I=0}|^2 &= \frac{|F_{K^+}|^2 + |F_{K^0}|^2}{2} - |F_{K^+}^{I=1}|^2, \\ \cos(\Delta\phi_{K^+}) &= \frac{|F_{K^+}|^2 - |F_{K^0}|^2}{2|F_{K^+}^{I=1}||F_{K^+}^{I=0}|}. \end{aligned} \quad (11)$$

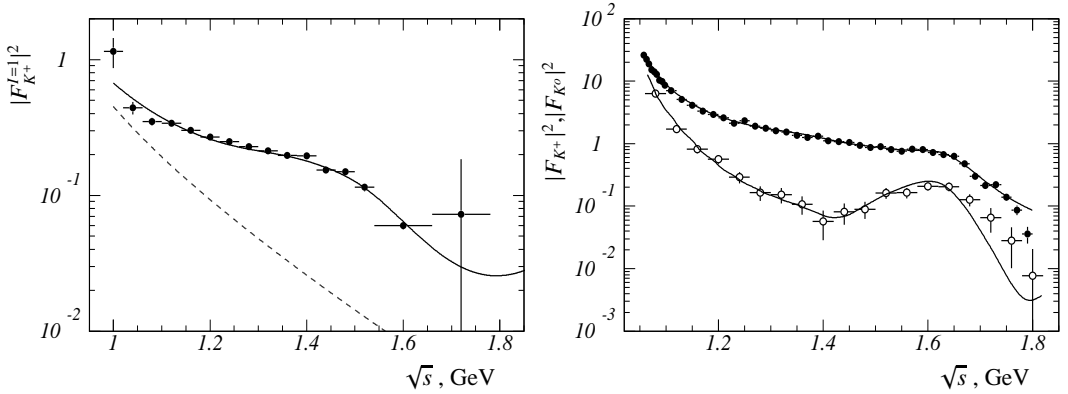


Figure 1. Left panel: The isovector kaon form factor squared obtained from the $\tau^- \rightarrow K^- K^0 \nu_\tau$ differential decay rate [8] as a function of \sqrt{s} . Right panel: The charged (open circles) and neutral (filled circles) kaon form factors squared obtained from the $e^+e^- \rightarrow K^+K^-$ [1] and $e^+e^- \rightarrow K_S K_L$ [2] cross section data respectively. In the both panels, the solid curves represent the results of the fit (Model II) described in the text. The dashed curve in the left panel shows the $\rho(770)$ contribution.

The isovector kaon form factor squared obtained using Eqs. (9,10) from the $\tau^- \rightarrow K^- K^0 \nu_\tau$ differential decay rate [8] is shown in Fig. 1(left). The τ measurement covers the energy region from $m_{K^-} + m_{K^0}$ to m_τ . This region is divided into two subregions, below and above 1.06 GeV, where the τ data should be treated in different way. Below 1.06 GeV the isoscalar form factor contains the resonance $\phi(1020)$, which width is significantly smaller than the bin width in Fig. 1(left). Above 1.06 GeV excited vector resonances contributing to the form factors have widths of about several hundred MeV. Therefore, we can use Eqs. (11) to calculate the form factors in each energy bin of the τ measurement without significant loss of information about their energy dependence.

The charged and neutral kaon form factors above 1.06 GeV are shown in Fig. 1(right). The neutral form factor is obtained using the the most precise and extensive data on the $e^+e^- \rightarrow K_S K_L$ cross section from the BABAR experiment [2]. The energy step in the $K_S K_L$ and τ measurements is the same (40 MeV) from 1.06 to 1.54 GeV. In the range 1.54-1.78 GeV corresponding the two last wide bins of τ data, we average over 3 bins. To obtain the charged form factor, the BABAR $e^+e^- \rightarrow K^+K^-$ data from Ref. [1] are used. The SND measurement of the $e^+e^- \rightarrow K^+K^-$ cross section [3] in the range 1.05-2.00 GeV having similar accuracy is in good agreement with the BABAR data. It should be noted that the accuracy of the $e^+e^- \rightarrow K^+K^-$ cross section is significantly higher than those for the $K_S K_L$ and τ measurements. In the energy region of interest the energy step of the K^+K^- measurement is 20 MeV. Therefore, in further calculations the K^+K^- data are averaged over 2 energy bins in the energy range 1.06 to 1.54 GeV, and over 6 bins in the range from 1.54 to 1.78 GeV, which corresponds the two last wide bins of τ data. The the $K_S K_L$ data in the latter range are averaged over 3 bins. The isoscalar kaon form and the cosine of the relative phase between the isoscalar and isovector form factors calculated using Eqs. (11) from e^+e^- and τ data are shown in Fig. 2.

Both isoscalar and isovector form factors decrease monotonically in the range below 1.4 GeV. This means that large contributions to the form factors come from the tails of the $\rho(770)$ in the isovector case, and $\omega(782)$ and $\phi(1020)$ in the isoscalar case. The latter two contributions are expected to interfere constructively [7], making the isoscalar form factor significantly larger than the isovector one. An unexpected feature of the form factors is the almost

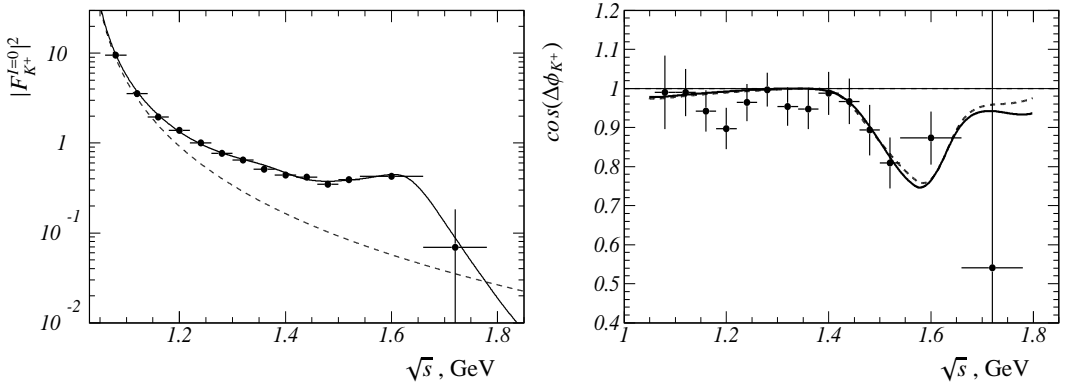


Figure 2. Left panel: The isoscalar kaon form factor squared calculated using Eqs. (11) from e^+e^- and τ data as a function of \sqrt{s} . The solid curve represents the results of the fit (Model II) described in the text. The dashed curve shows the $\omega(782)$ and $\phi(1020)$ contribution. Right panel: The cosine of the relative phase between the isoscalar and isovector form factors calculated using Eqs. (11) from e^+e^- and τ data. The dashed and solid curves represent the results of the fit with Model I and Model II described in the text, respectively.

constant, close-to-zero the phase difference between the isovector and isoscalar form factors in the energy range from 1.06 to 1.5 GeV. In this region, the resonances $\rho(1450)$ and $\omega(1420)$ are expected to give contributions to the form factors, which interfere with the very different $\rho(770)$ isovector and $\omega(782) + \phi(1020)$ isoscalar amplitudes. Above 1.5 GeV, resonance structures related to the $\rho(1700)$, $\omega(1650)$, and $\phi(1680)$ resonances are seen both in the energy dependences of the form-factor moduli and the phase difference.

The second part of this article is devoted to the simultaneous fitting of e^+e^- and τ two-kaon data in the framework of the vector meson dominance (VMD) model assuming isospin invariance and CVC. In this model, the amplitude of the single-photon transition $A_{\gamma^* \rightarrow K\bar{K}}$ is described as a sum of amplitudes of vector-meson resonances of the ρ , ω , and ϕ families.

The charged and neutral kaon cross sections are defined by the formulas (1) and (2). For description of the charged and neutral form factors we use parametrization from Ref. [7]:

$$F_{K^+}(s) = \frac{1}{2} \sum_{V=\rho,\rho',\dots} c_V BW_V + \frac{1}{6} \sum_{V=\omega,\omega',\dots} c_V BW_V + \frac{1}{3} \sum_{V=\phi,\phi',\dots} c_V BW_V, \quad (12)$$

$$F_{K^0}(s) = -\frac{1}{2} \sum_{V=\rho,\rho',\dots} c_V BW_V + \frac{1}{6} \sum_{V=\omega,\omega',\dots} c_V BW_V + \frac{1}{3} \sum_{V=\phi,\phi',\dots} c_V BW_V, \quad (13)$$

where the sums are taken over the resonances of the ρ , ω , or ϕ families, and the coefficients c_V are real. We fit to the cross-section data from the energy range below 2.1 GeV. The following resonances are included into the fit: $\rho(770)$, $\rho(1450)$, $\rho(1700)$, and $\rho(2150)$ denoted as ρ , ρ' , ρ'' , and ρ''' , respectively, $\omega(782)$, $\omega(1420)$, $\omega(1680)$, and $\omega(2150)$ denoted as ω , ω' , ω'' , and ω''' , respectively, $\phi(1020)$, $\phi(1680)$, and $\phi(2170)$ denoted as ϕ , ϕ' , and ϕ'' , respectively. The ρ''' , ω''' , and ϕ'' are needed to describe the measured cross-section energy dependences above 1.9 GeV. The partner of the $\rho(2150)$ resonance from the ω family is not observed yet. We introduce it into the fit with mass and width equal to those for $\rho(2150)$.

The resonance line shapes are described by the Breit-Wigner function

$$BW_V(s) = \frac{M_V^2}{M_V^2 - s - iM_V\Gamma_V(s)}, \quad (14)$$

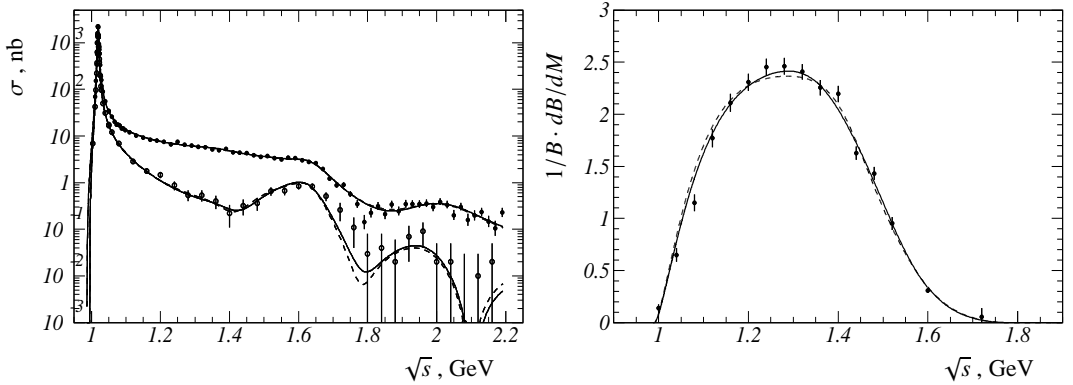


Figure 3. Left panel: The $e^+e^- \rightarrow K^+K^-$ and $e^+e^- \rightarrow K_S K_L$ cross sections. Right panel: The $\tau^- \rightarrow K^- K^0 \nu_\tau$ differential decay rate as a function of the K^-K^0 invariant mass. The dashed and solid curves represent the results of the fit with Model I and Model II described in the text, respectively.

where M_V and $\Gamma_V(s)$ are the resonance mass and energy dependent width. The widths for the ω and ϕ -mesons take into account all significant decay modes: $\pi^+\pi^-\pi^0$, $\pi^0\gamma$, and $\pi^+\pi^-$ for ω , and K^+K^- , $K_S K_L$, $\pi^+\pi^-\pi^0$, and $\eta\gamma$ for ϕ . For the $\rho(770)$, we take into account the main $\pi^+\pi^-$ decay mode and the contribution of the $\rho \rightarrow \omega\pi^0$ transition (see, for example, Ref. [12]) with the coupling constant $g_{\rho\omega\pi} = 15.9 \text{ GeV}^{-1}$ [13]. For excited vector meson widths, only one dominant channel is used: KK^* for ϕ -like resonances, $\omega\pi$ for ρ' , and $\rho\pi\pi$ for higher excited ρ states, $\rho\pi$ for ω' , and $\omega\pi\pi$ for higher excited ω states. The energy dependence of the partial widths are calculated using formulas from Refs. [14, 15].

The $\tau^- \rightarrow K^- K^0 \nu_\tau$ differential decay rate is described by Eq. (9) with the form factor

$$F_{K^-K^0}(s) = - \sum_{V=\rho,\phi',\dots} c_V B W_V. \quad (15)$$

The data sets on the $e^+e^- \rightarrow K^+K^-$ and $e^+e^- \rightarrow K_S K_L$ cross sections from CMD-3 [4, 5] in the ϕ -meson region, and from BABAR [1, 2] in the 1.06-2.16 GeV region are used in the fit. The BABAR K^+K^- data below 1.06 GeV are not included into the fit to avoid difficulties related to systematic difference in the ϕ -meson line shape and position between the CMD-3 and BABAR data sets.

The free fit parameters are the ϕ -meson mass and width, a parameter $\eta_\phi = g_{\phi K_S K_L} / g_{\phi K^+ K^-}$ describing the possible isospin-breaking difference between the $\phi \rightarrow K_S K_L$ and $\phi \rightarrow K^+ K^-$ decay constants, and eight parameters c_V . The parameters $c_{\rho''}$ and $c_{\phi''}$ are determined from the the conditions

$$\sum_{V=\rho,\phi',\dots} c_V = 1, \quad (16)$$

$$\frac{1}{3} \sum_{V=\omega,\omega',\dots} c_V + \frac{2}{3} \sum_{V=\phi,\phi',\dots} c_V = 1, \quad (17)$$

which provides the proper normalizations of the form factors $F_{K^+}(0) = 1$ and $F_{K^0}(0) = 0$. The parameter $c_{\omega''}$ is taken to be equal $c_{\rho''}$, as it is expected from the quark model [7]. The masses and widths of the ρ , ω , and the excited vector resonances are fixed to their nominal values [9]. During the fit they are allowed to vary within their uncertainties.

Table 1. The fitted values of the coefficients C_V in two models.

V	Model I	Model II
c_ρ	1.162 ± 0.005	1.067 ± 0.041
$c_{\rho'}$	-0.063 ± 0.014	-0.025 ± 0.008
$c_{\rho''}$	-0.160 ± 0.014	-0.234 ± 0.013
$c_{\rho'''} \equiv 1 - c_\rho - c_{\rho'} - c_{\rho''}$		0.063 ± 0.007
c_ω	1.26 ± 0.06	1.28 ± 0.14
$c_{\omega'}$	-0.13 ± 0.03	-0.13 ± 0.02
$c_{\omega''}$	-0.37 ± 0.05	$\equiv c_{\rho''}$
$c_{\omega'''} \equiv c_{\rho''}$		$\equiv c_{\rho''}$
c_ϕ	1.037 ± 0.001	1.038 ± 0.001
$c_{\phi'}$	-0.117 ± 0.020	-0.150 ± 0.009
$c_{\phi''} \equiv \frac{3}{2} - c_\phi - c_{\phi'} - \frac{1}{2} \sum_{V=\omega, \omega', \dots} c_V$		0.089 ± 0.015
χ^2/ν	199/143	183/142

The results of the fit are shown by the dashed curves (Model I) in Fig. 3 for the $e^+e^- \rightarrow K^+K^-$ and $e^+e^- \rightarrow K_S K_L$ cross sections and the $\tau^- \rightarrow K^- K^0 \nu_\tau$ differential decay rate, and in Fig. 2 (right) for the cosine of the relative phase between the isoscalar and isovector form factors. It is seen that the fitted curve does not reproduce well the shape of the τ -decay spectrum in Fig. 3 (right). Therefore, we perform another fit (Model II), in which the normalization constraints (16) and (17) are removed. Due to closeness of the ω'' and ϕ' masses the parameters $c_{\omega''}$ and $c_{\phi'}$ are strongly correlated and cannot be determined in Model II independently. Therefore, the additional constraint $c_{\omega''} = c_{\rho''}$ is introduced.

The results of the fit with Model II are shown in Figs. 1, 2 and 3 by the solid curves. This model describes the τ data significantly better and decreases the fit χ^2 by 16 units. The resulting $\chi^2/\nu = 183/142$, where ν is the number of degrees of freedom, is not quite good, but reasonable, taking into account that the systematic uncertainties of the measurements are not included into the fit. It should be also noted that the sizable contribution to the χ^2 (85 for 62 points) comes from the BABAR K^+K^- data, for which diagonal errors are used instead of the full error matrix. The sums on the left-hand sides of the normalization conditions (16) and (17) are calculated to be 0.87 ± 0.04 and 0.98 ± 0.05 , respectively. The 13% deviation from unity for the first sum indicates that the the description of the ρ -like resonance shapes, in particular the tail of the $\rho(770)$, in our fit model may be not quite correct. The difference in the parameters c_V between Model I and Model II may be used as an estimate of their model uncertainty.

The fitted value of the coefficient $\eta_\phi = 0.990 \pm 0.001$ is found to be consistent with unity. The η_ϕ value and fitted ϕ -meson mass and width, $M_\phi = 1019.461 \pm 0.004$ and $\Gamma_\phi = 4.248 \pm 0.006$ MeV, agrees well with the values of these parameters obtained in Refs. [4, 5]. The fitted values of the coefficients C_V are listed in Table 1. An interesting feature of the fits is a large deviation from the quark model predictions ($c_{\omega'} = c_{\rho'}$ and $c_{\omega''} = c_{\rho''}$) for excited ρ and ω resonances. These deviations are needed, in particular, to provide the almost constant value of the phase difference in the energy range 1.06–1.5 GeV, as it shown in Fig. 2(right).

We also perform a fit with an additional fit parameter α_{CVC} describing a possible deviation from the CVC hypothesis. This parameter is used as a scale factor to the τ data shown in Fig. 3(right). The fitted value of this parameter is $\alpha_{CVC} = 0.986(0.991) \pm 0.020$ for Model I (II). This shows that the CVC hypothesis for the $K\bar{K}$ system works with a few percent accuracy.

In conclusion, we have used recent precise measurements of the $e^+e^- \rightarrow K\bar{K}$ cross sections and the K^-K_S spectrum in the $\tau^- \rightarrow K^-K_S\nu_\tau$ decay to separate the isoscalar and isovector electromagnetic kaon form factors and determine the relative phase between them in a model independent way. The latter shows an unexpected energy dependence in the energy range from 1.06 to 1.5 GeV. It is almost constant and close to zero. We have simultaneously fitted to the $e^+e^- \rightarrow K^+K^-$ and $e^+e^- \rightarrow K_S K_L$ cross-section data and the hadronic mass spectrum in the $\tau^- \rightarrow K^-K_S\nu_\tau$ decay in the framework of the VMD model. The fit reproduces data reasonably well and shows that the CVC hypothesis for the $K\bar{K}$ system works with a few percent accuracy. To explain the specific energy dependence of the relative phase between the isoscalar and isovector form factors the large deviation from the quark model predictions for relations between the amplitudes of excited ρ and ω resonances is required.

This work is supported in part by the RFBR grants 16-02-00327-a.

References

- [1] J. P. Lees *et al.* (BABAR Collaboration), Phys. Rev. D **88**, 032013 (2013).
- [2] J. P. Lees *et al.* (BABAR Collaboration), Phys. Rev. D **89**, 092002 (2014).
- [3] M.N. Achasov *et al.*, (SND Collaboration), Phys. Rev. D **94**, 112006 (2016).
- [4] E. A. Kozyrev *et al.* (CMD-3 Collaboration), Phys. Lett. B **760**, 314 (2016).
- [5] E. A. Kozyrev *et al.* (CMD-3 Collaboration), Phys. Lett. B **779**, 64 (2018).
- [6] A. Hoefer, J. Gluza and F. Jegerlehner, Eur. Phys. J. C **24**, 51 (2002).
- [7] C. Bruch, A. Khodjamirian and J. H. Kuhn, Eur. Phys. J. C **39**, 41 (2005).
- [8] J. P. Lees *et al.* (BaBar Collaboration), Phys. Rev. D **98**, 032010 (2018).
- [9] M. Tanabashi *et al.* (Particle Data Group), Phys. Rev. D **98**, 030001 (2018).
- [10] M. Davier *et al.*, Eur. Phys. J. C **66**, 127 (2010).
- [11] M. Davier, S. Eidelman, A. Hocker and Z. Zhang, Eur. Phys. J. C **27**, 497 (2003).
- [12] M. N. Achasov *et al.* (SND Collaboration), Phys. Lett. B **486**, 29 (2000).
- [13] M. N. Achasov *et al.* (SND Collaboration), Phys. Rev. D **94**, 112001 (2016).
- [14] N. N. Achasov and A. A. Kozhevnikov, Phys. Rev. D **55**, 2663 (1997).
- [15] N. N. Achasov and A. A. Kozhevnikov, Phys. Rev. D **57**, 4334 (1998).